




Cite this: DOI: 10.1039/d6gc00351f

## Highly selective production of gasoline-range hydrocarbons *via* hydroconversion of polyolefins over Ru/CeO<sub>2</sub> and BEA hybrid catalysts

Junho Suh,<sup>a</sup> Hyeongdong Jung,<sup>a</sup> Joonkeol Yoon,<sup>a</sup> Jae-Soon Choi,<sup>b</sup> Jungup Bang<sup>b</sup> and Do Heui Kim \*<sup>a</sup>

To address the growing demand for sustainable plastic lifecycle, hydroconversion of polyolefins is a promising strategy for catalytic recycling of plastic wastes into fuel-range hydrocarbons. Ruthenium (Ru)-based hydrogenolysis catalysts exhibit high activity in the degradation of polyolefins, and bifunctional hydrocracking catalysts are much more beneficial for the selective production of gasoline-range hydrocarbons (C<sub>4</sub>–C<sub>12</sub>) than monofunctional hydrogenolysis catalysts. Herein, the Ru/CeO<sub>2</sub> and BEA zeolite hybrid catalyst demonstrated almost full conversion of low-density polyethylene (LDPE) with 95.4% gasoline selectivity, minimizing the production of low-value methane (<0.8%) in the hydroconversion of LDPE. Addition of BEA into Ru/CeO<sub>2</sub> switched the reaction pathway from hydrogenolysis to hydrocracking with a high fraction of branched hydrocarbons and efficient usage of hydrogen. The Ru/CeO<sub>2</sub> and BEA hybrid catalyst demonstrated the highest productivity of 3451 g<sub>C<sub>5</sub>–C<sub>12</sub></sub> g<sub>Ru</sub><sup>-1</sup> h<sup>-1</sup> among the recently reported Ru-based hydroconversion catalysts, and this was even higher than that of Pt- and Ir-based hydrocracking catalysts. The effect of BEA addition on the high gasoline selectivity was validated at a reaction temperature of 250 °C, and it was found that among the various physicochemical properties of the zeolite, the three-dimensional pore structure with a sufficient amount of surface acidity in the zeolite is crucial for the selective production of gasoline *via* LDPE hydroconversion. This work provides fundamental groundwork for designing bifunctional catalysts in polyolefin recycling.

Received 19th January 2026,  
Accepted 27th March 2026

DOI: 10.1039/d6gc00351f

rsc.li/greenchem

### Green foundation

1. This study advances green chemistry by chemically recycling polyolefin plastic wastes to produce gasoline-range hydrocarbons. This strategy reduces emission of toxic and harmful chemicals *via* landfilling and incineration, while yielding valuable fuels and chemicals under mild reaction conditions.
2. The Ru/CeO<sub>2</sub> and BEA hybrid catalyst converted almost all polyethylene into gasoline with 95.4% selectivity, minimizing the production of methane under 0.8% and maximizing the productivity of precious metals.
3. To make this work greener, future research should focus on substituting Earth-abundant metals for platinum-group metals and alleviating the effect of impurities in post-consumer plastic wastes.

## Introduction

Plastics are indispensable materials in our daily lives and in various industrial fields. However, as the mismanaged waste plastics accumulate and pollute the terrestrial and marine ecosystems, the United Nations has declared plastics to be one of the significant environmental menaces faced by the world.<sup>1,2</sup> Only about 10% of plastics are recycled among

more than 7000 Mt of end-of-life plastic wastes, and most of the plastics recycled are mechanically recycled with a downgrade of their properties.<sup>3</sup> Polyolefins including low and high density polyethylene (LDPE and HDPE) and polypropylene (PP) are widely used plastics with excellent properties, especially in packaging, and they compose about 60% of waste plastics due to their short functional life.<sup>4</sup> The pyrolysis-based strategy is widely recognized as an efficient and economical technique for the global plastic waste challenge,<sup>5,6</sup> and catalytic hydroconversion is a kind of solution *via* chemical recycling to tackle the big threat of polyolefin plastic wastes. Hydroconversion is an advantageous process compared to the conventional pyrolysis: it requires a

<sup>a</sup>School of Chemical and Biological Engineering, Institute of Chemical Processes, Seoul National University, 1 Gwanak-ro, Gwanak-Gu, Seoul 08826, Republic of Korea

<sup>b</sup>Catalyst R&D, LG Chem., 188 Munji-ro, Yuseong-gu, Daejeon 34122, Republic of Korea



milder reaction temperature of 200–300 °C, has high selectivity toward liquid products, and is carried out without any solvents.<sup>7</sup> In addition, pyrolysis is often followed by upgrading processes such as additional hydrocracking, isomerization, and hydrotreating, which require metal catalysts and pressurized hydrogen.<sup>8</sup> On the other hand, hydroconversion proceeds in minimized steps and the desired short-chain hydrocarbons can be produced without the post-treatment processes.

Gasoline-range hydrocarbons ( $C_4$  to  $C_{12}$ ) are highly usable in human life and various industries. We considered  $C_4$ – $C_{12}$  range hydrocarbons as gasoline in this research because branched  $C_4$  and  $C_5$  are frequently incorporated as gasoline additives to adjust volatility and improve cold-start performance.<sup>9,10</sup> They represent one of the most essential fractions in the modern fuel pool, owing to their direct use as transportation fuels and blending components in commercial gasoline. Global energy statistics consistently highlight the dominance of gasoline consumption in the liquid fuel sector; for example, according to the International Energy Agency (IEA), gasoline accounted for approximately 25–30% of total oil demand for road transport in 2022.<sup>11</sup> This demand is projected to remain significant in the coming decades despite the gradual penetration of electrification, due to the existing internal combustion vehicle fleet and the necessity of high-octane blending components.<sup>12</sup> In addition, gasoline-range hydrocarbons could be directly utilized in current petrochemical processes for the production of various valuable chemicals and plastics. In particular, global trends in plastic production require mandatory recycled contents for single-use plastic bottles and plastic packaging.<sup>13,14</sup> From a perspective of resource sustainability, production of  $C_4$ – $C_{12}$  hydrocarbons through hydroconversion of polyethylene and polypropylene has attracted growing attention.

In recent years, PGM-based catalysts have been studied in hydroconversion of long-chain polyolefins into shorter hydrocarbons, including gasoline ( $C_4$ – $C_{12}$ ), jet fuel ( $C_8$ – $C_{16}$ ), diesel ( $C_{13}$ – $C_{20}$ ), and lubricants ( $C_{21}$ – $C_{36}$ ).<sup>15–21</sup> Ceria ( $CeO_2$ )-supported Ru catalysts are especially active hydrogenolysis catalysts, and some researchers are attempting to improve the catalytic properties of Ru/ $CeO_2$  catalysts such as the structure of Ru particles and the  $CeO_2$  support.<sup>15,22,23</sup> Nevertheless, Ru/ $CeO_2$  demonstrates broad liquid product distribution with a huge amount of low-value methane due to the excessive hydrogenolysis activity of Ru. To improve the selectivity of liquid products and suppress the production of methane, bifunctional hydrocracking catalysts can be utilized by the introduction of acid sites over the support or acidic promoters.<sup>19,24–27</sup> One simple method to prepare bifunctional catalysts is to mix pristine acidic catalysts such as zeolites with metal catalysts, combining the functional properties of different catalysts for synergistic performance without changing their physicochemical properties and economizing the usage of metals.<sup>28,29</sup> It was reported that the activity of Pt-based catalysts was greatly enhanced when they were mixed with BEA and Y zeolites.<sup>30,31</sup> However, the catalytic activity of mixture catalysts with

Ru-based catalysts and zeolites has not been much reported so far.

In this study, we focus on the synergistic effect between Ru/ $CeO_2$  and BEA-type zeolite on the hydroconversion of LDPE. Due to the synergistic effect of Ru/ $CeO_2$  and BEA, LDPE was successfully converted into gasoline-range hydrocarbons with excellent selectivity and suppressed production of methane. Various reaction parameters including reaction temperature, reaction time, and mixing ratio of Ru/ $CeO_2$  to BEA in the hybrid catalyst were evaluated. In addition, the effect of catalytic parameters such as surface acidity, the pore diameter of the zeolite, and the proximity of metal sites and acid sites was investigated, and the optimum combination of the hybrid catalyst was a  $CeO_2$ -supported Ru catalyst mixed with the pristine BEA zeolite. Finally, the flexibility of the hybrid catalyst's hydroconversion activity toward various types of PE and PP feeds was discussed.

## Results and discussion

### Synergistic effect of the Ru/ $CeO_2$ and BEA hybrid catalyst on LDPE hydroconversion

Catalyst characterization data including powder X-ray diffraction (XRD), high resolution transmission electron microscopy (HRTEM), and  $N_2$  adsorption–desorption of Ru/ $CeO_2$ , BEA, and the Ru/ $CeO_2$  + BEA hybrid catalyst are summarized in Fig. S1 and Table S1. XRD of Ru/ $CeO_2$  + BEA shows characteristic peaks of both Ru/ $CeO_2$  and BEA, and the Cs-TEM image of Ru/ $CeO_2$  + BEA shows a mixed phase of Ru/ $CeO_2$  and BEA. Also, BET analysis using  $N_2$  adsorption–desorption shows that Ru/ $CeO_2$  + BEA has a medium surface area, pore diameter and pore volume of Ru/ $CeO_2$  and BEA. According to the characterization data, Ru/ $CeO_2$  + BEA shows characteristic properties of Ru/ $CeO_2$  and BEA and physical mixing of Ru/ $CeO_2$  with BEA does not cause any changes in the physicochemical properties of Ru/ $CeO_2$  and BEA, respectively.

The catalytic activity of Ru/ $CeO_2$  (Ru loading = 5 wt%) and BEA(25) zeolite in LDPE hydroconversion is shown in Fig. 1 and Table S2. As shown in Fig. 1a and b, Ru/ $CeO_2$  is an active hydrogenolysis catalyst, converting almost all polymers into liquid ( $C_4$ – $C_{36}$ ) and gaseous products ( $C_1$ – $C_3$ ) with 84.2% and 15.7% selectivity, respectively. However, the excessive hydrogenolysis activity of Ru/ $CeO_2$  results in 12.0% of low-value methane ( $C_1$ ) and liquid products with broad distribution, which indicates that external C–C bond cleavage is dominant over internal C–C bond scission.<sup>15</sup> BEA zeolite is a commercial cracking catalyst and widely used in catalytic pyrolysis processes. However, the LDPE degradation activity of BEA(25) was low due to a mild reaction temperature of 260 °C, although the main products are gasoline-range hydrocarbons ( $C_4$ – $C_{12}$ ), indicating the cracking activity of long chains into shorter chains.

The hybrid catalyst of Ru/ $CeO_2$  and BEA showed improved activity in PE hydroconversion with an LDPE conversion of 98.8%, a gasoline-range hydrocarbon selectivity of 95.4%, and a suppressed  $C_1$  yield of 0.8%, while using only one-third of



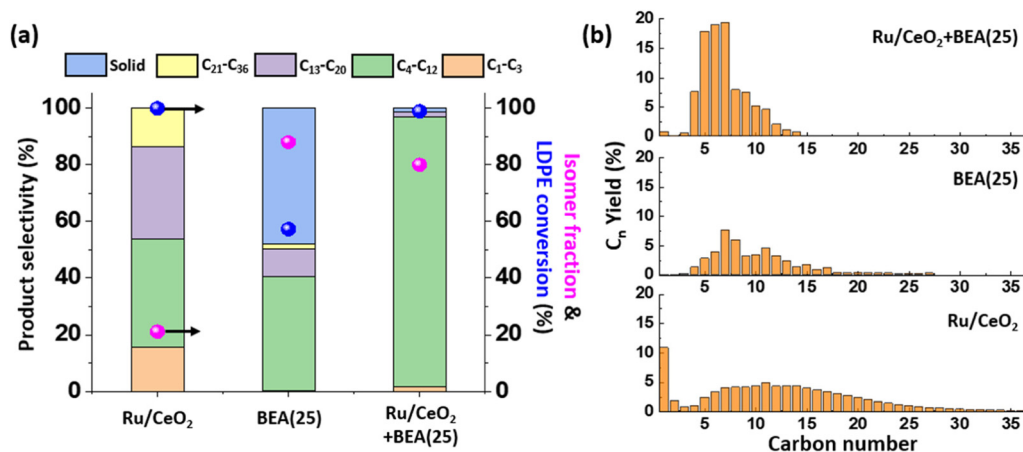


**Fig. 1** (a) Product selectivity, LDPE conversion and isomer fraction in the gas and liquid products, and (b) product distribution over Ru/CeO<sub>2</sub>, BEA(25), and Ru/CeO<sub>2</sub> + BEA(25) catalysts (mass ratio of Ru/CeO<sub>2</sub> to BEA(25) = 1 : 2). Reaction conditions: 3.5 g of LDPE, 0.25 g of catalysts, 260 °C, 50 bar H<sub>2</sub>, 4 h.

the Ru metal compared to Ru/CeO<sub>2</sub> (Fig. 1a, b and Table S2). Likewise, at a lower PE/catalyst ratio and lower reaction temperature, LDPE was successfully converted into gasoline with high selectivity and low methane yield when the reaction time was extended to 16 h (Fig. S2). Catalysts without supported Ru metal such as CeO<sub>2</sub> and CeO<sub>2</sub> + BEA(25) exhibited very low activity in polyethylene hydroconversion (Fig. S3), indicating that Ru metal is an essential component in the Ru/CeO<sub>2</sub> + BEA hybrid catalyst. Although the polymer degradation activity of BEA was very low due to the low reaction temperature, LDPE conversion and gasoline selectivity were significantly increased when BEA was mixed with Ru/CeO<sub>2</sub>. Compared to the hydroconversion activity of Ru/CeO<sub>2</sub>, the excessive hydrogenolysis activity of Ru/CeO<sub>2</sub> that produces methane seems to be suppressed over Ru/CeO<sub>2</sub> + BEA. Such a decrease in methane yield indicates that the reaction pathway is switched from hydrogenolysis to hydrocracking. At the same time, BEA mainly cleaves the C-C bonds of hydrocarbon chains and selectively yields gasoline-range hydrocarbons *via* the hydrocracking mechanism. Through the change of reaction pathway from hydrogenolysis to hydrocracking and synergistic cooperation of Ru/CeO<sub>2</sub> and BEA, LDPE could be successfully converted into gasoline over the hybrid catalyst with high selectivity and suppressed methane production.

In addition to the excellent gasoline selectivity, isomer fraction is another factor that indicates the synergistic effect of the Ru/CeO<sub>2</sub> + BEA catalyst. Most of the products from PE degradation over Ru/CeO<sub>2</sub> were linear hydrocarbons, calculated as 21.1% isomer fraction (Fig. 1a and Table S2). Conversely, Ru/CeO<sub>2</sub> + BEA led to an increased portion of branched hydrocarbon products up to 79.9%, since the C-C bond cleavage occurs mainly through the repeated process of isomerization and  $\beta$ -scission over the acid sites of BEA zeolite.<sup>32</sup> A high proportion of branched hydrocarbons in gasoline could increase the octane rating, one of the critical properties of a gasoline fuel's resistance to knock or to ignite prematurely.<sup>33</sup> Moreover,

when the highly isomerized gasoline-range hydrocarbons are directly used in the naphtha cracking center, production of versatile propylene could be increased.<sup>34</sup> Meanwhile, hydrogen conversion was as high as 70.8% in Ru/CeO<sub>2</sub> but significantly decreased to 40.3% in the hybrid catalyst, indicating that hydrogen is effectively utilized to produce gasoline-range hydrocarbons instead of methane. It can be suggested from these results that the synergistic effect of (de)hydrogenation by Ru/CeO<sub>2</sub> and isomerization-cracking by BEA in the hybrid catalyst could not only enhance gasoline selectivity with a high fraction of branched hydrocarbons but also reduce the usage of expensive precious metals and hydrogen.

The effect of the LDPE to catalyst ratio in the hydroconversion over Ru/CeO<sub>2</sub> + BEA is shown in Fig. S4. LDPE conversion was set to the medium range from 70% to 78%. At a higher LDPE to catalyst ratio of 28, a relatively long reaction time of 12 h was required to depolymerize 70% of the initial LDPE, whereas a shorter reaction time of 4 h was required to convert LDPE into shorter hydrocarbons at higher LDPE to catalyst ratios of 14 and 10. According to the isomer fraction, selective hydrocracking to gasoline-range hydrocarbons was observed in LDPE/catalyst ratios of 28 and 10, and at an LDPE/catalyst ratio of 14, the synergistic effect of Ru/CeO<sub>2</sub> and BEA to yield gasoline was weak. Based on these results, we decided to conduct the hydroconversion reaction at a relatively high reaction temperature (260 °C) and long reaction time (4 h) to effectively show the catalytic performance of Ru/CeO<sub>2</sub> + BEA and the synergistic effect of Ru/CeO<sub>2</sub> and BEA.

#### Mass ratio of Ru/CeO<sub>2</sub> and BEA and Ru loading effect in the hybrid catalyst

To further investigate the leverage of Ru/CeO<sub>2</sub> and BEA fractions in the dual catalyst, catalytic activity according to the different mixing ratios was examined and is shown in Fig. 2a. Addition of a small amount of BEA into Ru/CeO<sub>2</sub> in a 3 : 1 catalyst resulted in only a slight increase in gasoline yield and



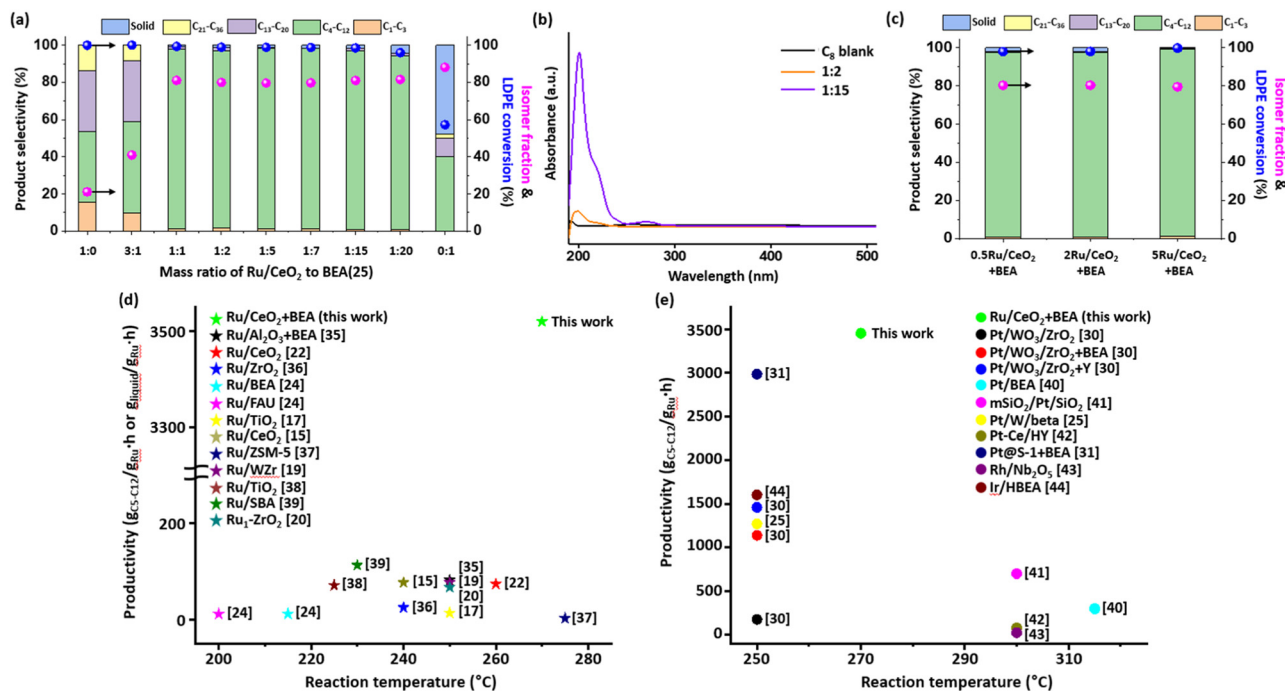


**Fig. 2** (a) Product selectivity, LDPE conversion and isomer fraction in the gas and liquid products over Ru/CeO<sub>2</sub> + BEA (25) with different mixing ratios. (b) UV-vis spectroscopy spectra of liquid products from LDPE hydroconversion. Reaction conditions: 3.5 g of LDPE, 0.25 g of catalysts, 260 °C, 50 bar H<sub>2</sub>, 4 h. (c) Product selectivity, LDPE conversion and isomer fraction in the gas and liquid products over Ru/CeO<sub>2</sub> + BEA(25) with different Ru loadings. Reaction conditions: 3.5 g of LDPE, 0.25 g of catalysts, 270 °C, 50 bar H<sub>2</sub>, 2 h. (d and e) Catalytic hydroconversion performance of (d) Ru-based catalysts and (e) Pt, Rh, and Ir-based catalysts in recently reported literature studies.

isomer fraction, and the extent of decrease in methane yield was low, implying that the hydrogenolysis pathway is dominant over the hydrocracking pathway. As the proportion of Ru/CeO<sub>2</sub> decreased and that of BEA increased until a mixing ratio of 1:15, high levels of gasoline yield and branched product fraction were maintained. Methane yield over the hybrid catalysts gradually decreased from 0.88% at 1:1 to 0.06% at 1:15 in accordance with the decreased amount of Ru. Nevertheless, nearly full conversion of LDPE with 95–97% of both gasoline selectivity and isomer fraction could be achieved through the synergistic activity of Ru/CeO<sub>2</sub> and BEA. These results indicate that the mixture catalyst of Ru/CeO<sub>2</sub> and BEA has the outstanding advantage of minimizing the usage of expensive Ru in the production of gasoline-range hydrocarbons from LDPE chemical recycling. However, a too low fraction of Ru/CeO<sub>2</sub> in the 1:20 catalyst led to an increase in solid residue (4.0%). Therefore, a minimum amount of Ru is essential for the complete conversion of LDPE.

In addition, an optimum amount of Ru is important to ensure high quality of gasoline from LDPE hydroconversion. Olefins in gasoline fuel increase the possibility of knocking, decrease the combustion efficiency to increase incomplete combustion, and readily react with oxygen in the air to form gums, causing clogging and sticking in engine systems.<sup>35</sup> In addition, olefins or aromatics reduce the quality of the recycled naphtha, influencing process severity in the naphtha cracking center (NCC) when directly put into the reactor.<sup>36</sup> As

shown in Fig. S5, the extracted liquid products in toluene are colorless at mass ratios of Ru/CeO<sub>2</sub> to BEA between 3:1 and 1:7. The smaller the amount of Ru/CeO<sub>2</sub> introduced into the mixture catalyst, the more yellowish the color of the collected liquid products, which implies the possibility of containing olefins and aromatics in the liquid products. In some molecules that have unsaturated carbon-carbon bonds, which can conjugate with each other, they can show a light yellowish color.<sup>37</sup> It is reported that unsaturated hydrocarbons such as olefins and aromatics produced from the cracking of long-chain hydrocarbons might have one or more C=C double bonds and can exhibit a yellowish color.<sup>38</sup> Actually, an octadecene (C<sub>18</sub><sup>−</sup>) solution dissolved in octane (C<sub>8</sub>) is transparent, but model liquid products extracted from the cracking of C<sub>18</sub><sup>−</sup> under the BEA catalyst turned yellow (Fig. S6). In addition to the color of the liquid, UV-vis spectroscopy is one of the characterization methods that can detect the presence of unsaturated hydrocarbons in the solution.<sup>20,39</sup> The absorption peak of  $\pi \rightarrow \pi^*$  electronic transition in C=C bonds of olefins is known to occur at  $\lambda_{\max}$  of ~190 nm, while those in aromatics could be assigned between 250 nm and 280 nm. These  $\lambda_{\max}$  values of absorption peaks could increase to higher wavelengths if the olefins and aromatics have two or more conjugated C=C bonds. In fact, a C<sub>8</sub> paraffin solution with all saturated C-C bonds showed an absorption peak for C-C bonds under 180 nm, while C=C bonds of C<sub>18</sub><sup>−</sup> in the C<sub>8</sub> solution absorbed UV light around 200 nm. Liquid products from the



degradation of  $C_{18}^{=}$  under the BEA catalyst represented broad absorption peaks between 200 nm and 400 nm, which originated from conjugated C=C bonds of olefins and aromatics. This confirms that the yellowish color of the liquid is related to the presence of olefins and aromatics. After determining the existence of olefinic and aromatic hydrocarbons based on the color of the solution and UV-vis spectroscopy, transparent and yellowish liquid products of LDPE hydroconversion over Ru/CeO<sub>2</sub> + BEA are analyzed with UV-vis spectroscopy (Fig. 2b). Absorption peaks of transparent liquid products at 200 nm over the 1:2 catalyst remained low, implying that the production of unsaturated hydrocarbon is minimized by the active hydrogenation of Ru/CeO<sub>2</sub>. On the other hand, yellowish liquid products of the 1:15 catalyst showed an intense peak near 200 nm and broad shoulder peaks between 200–250 nm and 250–300 nm. It can be inferred that more olefinic and aromatic hydrocarbons are present in the liquid product of the 1:15 catalyst due to the low hydrogenation activity. These results propose that an optimum ratio of Ru/CeO<sub>2</sub> and BEA in the hybrid catalyst is critical for ensuring not only high LDPE conversion but also high quality of gasoline products. We concluded that a mixing ratio of 1:2 is the optimum ratio over the hybrid catalyst in this study.

The effect of Ru loading in the dual catalyst on LDPE hydroconversion was determined as shown in Fig. 2c. Since the total amount of the hybrid catalyst and the mass ratio of Ru/CeO<sub>2</sub> and BEA were fixed at 0.25 g with Ru/CeO<sub>2</sub>:BEA = 1:2, the decrease in the weight percent of Ru in Ru/CeO<sub>2</sub> is directly related to the reduced amount of Ru introduced into the hydroconversion reaction. Nevertheless, Ru/CeO<sub>2</sub> + BEA exhibited excellent performance in selective gasoline production at 270 °C and 2 h under the low Ru loading. When the loading of Ru was decreased from 5 wt% to 0.5 wt%, the yield of the solid residue slightly increased from 0.1% to 2.0%, but the high levels of gasoline selectivity and isomer fraction were maintained at 98–97% and 79–80%, respectively. A reduced amount of Ru introduced into the hydroconversion reaction could result in decreased LDPE conversion; however, the strong synergy between Ru/CeO<sub>2</sub> and BEA was effective in LDPE hydroconversion, yielding gasoline-range hydrocarbons with excellent selectivity. This indicates that the expense of precious Ru metal could be saved through the strong synergistic effect between low loading Ru/CeO<sub>2</sub> and BEA.

Based on the above results, the productivity of the Ru/CeO<sub>2</sub> and BEA hybrid catalyst in hydroconversion of polyolefins was compared with recently reported literature studies on PGM-based catalysts as shown in Fig. 2d.<sup>15,17,19,20,22,24,25,30,31,40–49</sup> Detailed information of the catalytic hydroconversion activity is summarized in Tables S3 and S4. For reasonable comparison among the catalysts, productivity was calculated based on either C<sub>5</sub>–C<sub>12</sub> range hydrocarbons from hydrocracking catalysts or liquid products from hydrogenolysis catalysts. Most Ru-based catalysts such as Ru/CeO<sub>2</sub>, Ru/TiO<sub>2</sub>, Ru/ZrO<sub>2</sub>, Ru/BEA, Ru/FAU and Ru/ZSM-5 are specialized in hydrogenolysis and they produce a large amount of light alkanes and liquid products with broad carbon number distribution, yielding low

productivity from 3 to 77 g<sub>liquid</sub> g<sub>Ru</sub><sup>-1</sup> h<sup>-1</sup>. Ru-based bifunctional catalysts such as Ru/WZr, Ru/SBA and Ru/Al<sub>2</sub>O<sub>3</sub> + BEA exhibit improved selectivity towards C<sub>5</sub>–C<sub>12</sub> range hydrocarbons. However, the C<sub>5</sub>–C<sub>12</sub> productivity was still low in the range of 77–113 g<sub>C<sub>5</sub>–C<sub>12</sub></sub> g<sub>Ru</sub><sup>-1</sup> h<sup>-1</sup>, possibly due to the high loading of Ru. Our Ru/CeO<sub>2</sub> + BEA hybrid catalyst shows excellent hydrocracking performance even under a low Ru loading of 0.5 wt% and the C<sub>5</sub>–C<sub>12</sub> productivity was 3451 g<sub>C<sub>5</sub>–C<sub>12</sub></sub> g<sub>Ru</sub><sup>-1</sup> h<sup>-1</sup>, 30-fold higher than the previous top productivity of 113 g<sub>C<sub>5</sub>–C<sub>12</sub></sub> g<sub>Ru</sub><sup>-1</sup> h<sup>-1</sup> in Ru/SBA. Moreover, the productivity of the Ru/CeO<sub>2</sub> + BEA catalyst toward C<sub>5</sub>–C<sub>12</sub> range hydrocarbons was higher than that of Pt, Rh, and Ir-based catalysts. Pt-based hydrocracking catalysts with low Pt loading, such as Pt/WO<sub>3</sub>/ZrO<sub>2</sub> + Y, Pt/W/beta, and Pt@S-1 + BEA, demonstrated high levels of C<sub>5</sub>–C<sub>12</sub> productivity from 1272 to 2983 g<sub>C<sub>5</sub>–C<sub>12</sub></sub> g<sub>Pt</sub><sup>-1</sup> h<sup>-1</sup>. The productivities of the Rh-based catalyst (Rh/Nb<sub>2</sub>O<sub>5</sub>) and the Ir-based catalyst (Ir/HBEA) were 26 g<sub>C<sub>5</sub>–C<sub>12</sub></sub> g<sub>Rh</sub><sup>-1</sup> h<sup>-1</sup> and 1604 g<sub>C<sub>5</sub>–C<sub>12</sub></sub> g<sub>Ir</sub><sup>-1</sup> h<sup>-1</sup>, respectively. Our Ru/CeO<sub>2</sub> + BEA hybrid catalyst exhibited a higher productivity of 3451 g<sub>C<sub>5</sub>–C<sub>12</sub></sub> g<sub>Ru</sub><sup>-1</sup> h<sup>-1</sup> compared to that of the previous Pt, Rh, and Ir-based catalysts, and considering the market price of each metal, the productivity of our dual catalyst was much higher than that of other PGM-based catalysts. Considering the metal price, the Ru/CeO<sub>2</sub> + BEA hybrid catalyst demonstrated the highest productivity of 71 g<sub>C<sub>5</sub>–C<sub>12</sub></sub> per \$<sub>metal</sub> per h, while the previous top productivity in the literature was 42 g<sub>C<sub>5</sub>–C<sub>12</sub></sub> per \$<sub>metal</sub> per h in Pt@S-1 + BEA. These results indicate that our Ru/CeO<sub>2</sub> + BEA hybrid catalyst could produce a much greater amount of C<sub>5</sub>–C<sub>12</sub> range hydrocarbons *via* LDPE hydroconversion at the same cost of precious metals.

### Effect of reaction temperature on LDPE hydroconversion over Ru/CeO<sub>2</sub> and the hybrid catalyst

Fig. 3 shows the effect of BEA addition to Ru/CeO<sub>2</sub> on LDPE hydroconversion at different reaction temperatures. Without BEA, Ru/CeO<sub>2</sub> catalyzed almost all LDPE into gasoline, diesel, lubricant range and gaseous hydrocarbons with a methane yield of 11–12% across the reaction temperature range of 240–260 °C. Ru/CeO<sub>2</sub> was an active hydrogenolysis catalyst but produced a large amount of methane and a broad carbon number distribution in the liquid products from C<sub>4</sub> to C<sub>36</sub>, with a low isomer fraction under 20%. When BEA was mixed with Ru/CeO<sub>2</sub> at 240 °C, LDPE conversion significantly dropped to 41% and the solid residue was mainly obtained due to the reduced amount of Ru/CeO<sub>2</sub> to one-third. At an elevated reaction temperature of 250 °C, LDPE conversion increased to 78% but a considerable amount of solid residue was still left unreacted and the product distribution was broad. In the Ru/CeO<sub>2</sub> + BEA catalyst, both Ru metal and external acid sites of BEA zeolite could contribute to the initial decomposition of LDPE. It can be inferred that a reaction temperature below 250 °C is insufficient for the external acid sites of BEA to activate the initial LDPE, and the decreased amount of Ru introduced is directly related to the reduced LDPE conversion. Also, the isomer fraction in the hydroconversion products was 32–42% at 240–250 °C, indicating that the isomerization



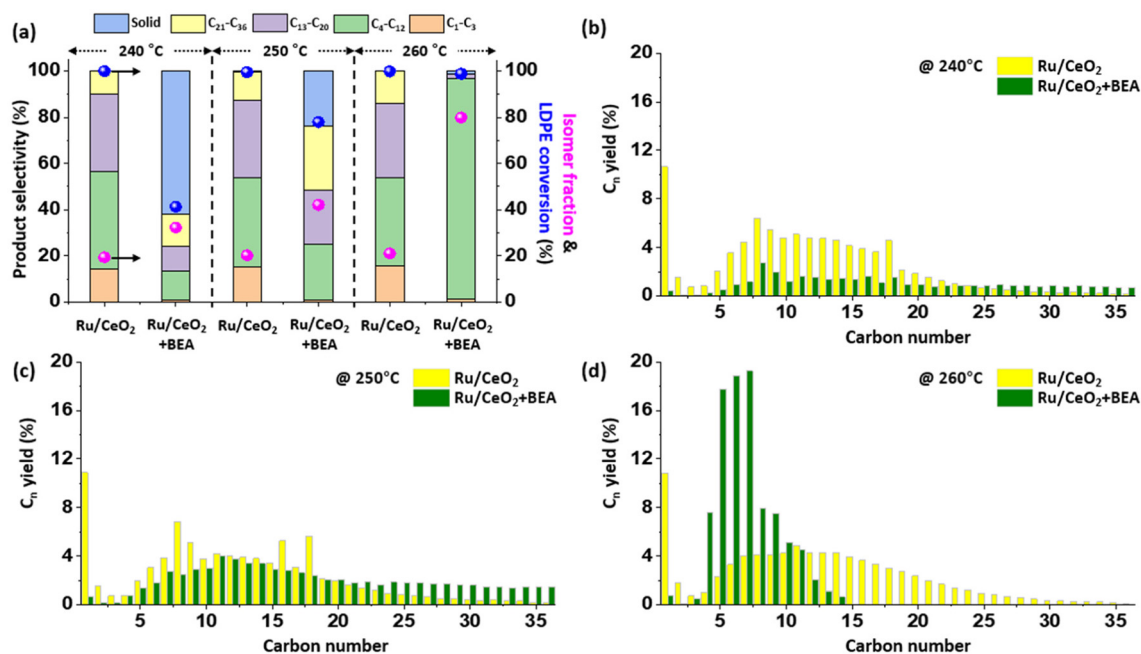


**Fig. 3** (a) Product selectivity, LDPE conversion and isomer fraction in the gas and liquid products, and product distribution at (b) 240 °C, (c) 250 °C, and (d) 260 °C. Reaction conditions: 3.5 g of LDPE, 0.25 g of catalysts, 50 bar H<sub>2</sub>, 4 h, mixing ratio of Ru/CeO<sub>2</sub> to BEA = 1 : 2.

activity of BEA was low and the degradation of LDPE proceeded primarily *via* the hydrogenolysis mechanism. It is reported that the addition of BEA could slow down the hydroconversion reaction at 240 °C due to weak isomerization activity<sup>50</sup> and competitive adsorption of reactants (dilution effect) when mixed with Ru/CeO<sub>2</sub>. When the reaction temperature was further increased to 260 °C, the hybrid catalyst decomposed almost all LDPE into gasoline-range hydrocarbons with an excellent selectivity of 95% and an improved isomer fraction of 80%. In spite of the smaller amount of Ru catalyst used, hydroconversion of LDPE was promoted to produce gasoline through the change of the reaction pathway from hydrogenolysis over Ru/CeO<sub>2</sub> to hydrocracking over BEA.

In addition, the catalytic performance of the mixture catalyst according to the reaction temperature was also examined at sufficient reaction time, as shown in Fig. S7. For the adequate comparison of catalytic activity, LDPE conversion under each catalyst was set to 90–100%. In Ru/CeO<sub>2</sub> + BEA catalysts at all reaction temperatures, introduction of BEA resulted in the decreased production of methane, demonstrating that the alkylcarbenium ions are stabilized in BEA through the bimolecular mechanism so that the production of methane, ethane, and ethylene is suppressed.<sup>34</sup> At a mild reaction temperature of 230 °C, the addition of BEA slightly reduced LDPE conversion and did not induce an increase in isomer fraction, indicating that BEA was inactive in both the initiation of LDPE decomposition and the selective production of gasoline at the low reaction temperature. When the reaction temperature was increased to 240 °C, Ru/CeO<sub>2</sub> + BEA showed a slight improvement, with the isomer fraction doubling from 13.6% to 26.6%, which proves a partial hydrocracking pathway over the mixture cata-

lyst. Nevertheless, hydroconversion of LDPE mainly proceeded with hydrogenolysis with a broad carbon number range from gasoline to diesel and lubricants. Above 250 °C, the fundamental hydroconversion mechanism over the hybrid catalyst switched to hydrocracking and the gasoline selectivity was rapidly increased to 77.9% with a tripled fraction of branched products (57.3%) compared to Ru/CeO<sub>2</sub> (18.9%). When the reaction temperature was further increased to 260 °C, gasoline-range products were much more concentrated with C<sub>5</sub>–C<sub>7</sub> alkanes but the isomer fraction in the products was maintained at a maximum value of 57% and the selectivity toward gasoline was 76.5%, similar to the gasoline selectivity at 250 °C. On the other hand, the selectivity of diesel-range products decreased and gas product selectivity increased, indicating the external C–C bond cleavage by Ru/CeO<sub>2</sub> at an extended reaction time even in the presence of BEA. To sum up the effect of reaction temperature on the hybrid catalysts, addition of BEA to Ru/CeO<sub>2</sub> affected the product distribution and isomer fraction from 240 °C by switching the reaction pathway from hydrogenolysis to hydrocracking. A minimum reaction temperature of 260 °C is important to maximize the selectivity of gasoline and isomer fraction because skeletal rearrangement must precede for vigorous C–C bond scission in hydrocracking and skeletal rearrangement is reported to be highly temperature-dependent.<sup>51</sup> A low reaction temperature of 250 °C could be effective in the case of sufficient reaction time.

#### Effect of reaction time and hydrogen pressure on LDPE hydroconversion over the hybrid catalyst

The influence of reaction time is shown in Fig. 4. Over the Ru/CeO<sub>2</sub> + BEA catalyst at 260 °C, the catalytic activity was low in



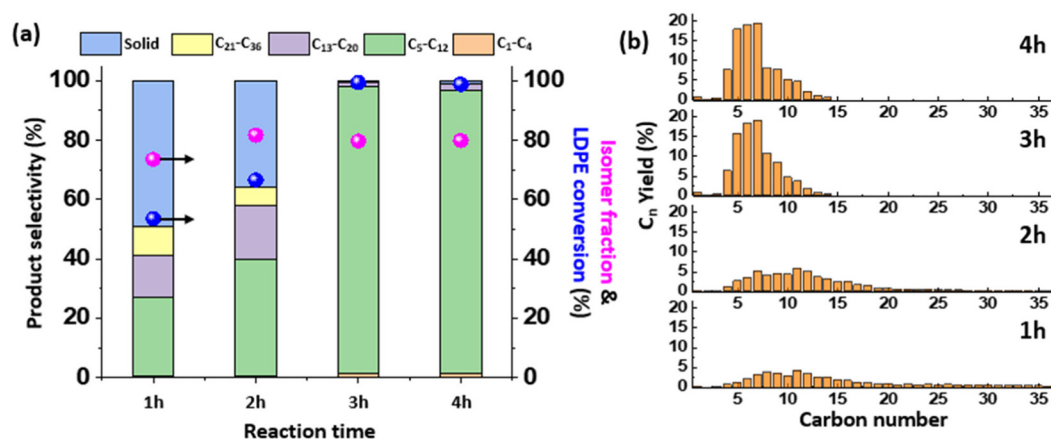


Fig. 4 (a) Product selectivity, LDPE conversion and isomer fraction in the gas and liquid products, and (b) product distribution according to the reaction time. Reaction conditions: 3.5 g of LDPE, 0.25 g of catalysts, 260 °C, 50 bar H<sub>2</sub>, 1–4 h, mixing ratio of Ru/CeO<sub>2</sub> to BEA = 1 : 2.

the early phase of hydroconversion and most of the LDPE reactants remained residual solid. LDPE conversion and gasoline selectivity were 54% and 25% at 1 h, and they increased to 67% and 37%, respectively, until 2 h. Deconstruction of LDPE in the early stage is promoted in a highly viscous liquid melt; thus the initial activity of the dual catalyst might be low due to the diffusion resistance and consequential lack of isomerized reaction intermediates. Also, it is reported that the adsorption free energy is higher in the melt of larger hydrocarbons.<sup>52</sup> After 2 h, the catalytic performance of the hybrid catalyst suddenly jumped, with the yield of solid residue and gasoline selectivity reaching 0.6% and 97%. As the viscous liquid hydrocarbons are gradually converted into lighter products, the viscosity of the liquid melts in the reactor decreases, and in accordance with the following mass transfer increase, residual polymers in the reactor could be quickly degraded to short-chain hydrocarbons. In addition, the isomer fraction at 1 h was 73% and it reached a saturated level of about 80% at 2 h, which seems enough for the following active  $\beta$ -scission *via* hydrocracking. After the sudden increase in hydroconversion activity, the product yield seemed to equilibrate and there were no noticeable changes in product distribution at 4 h. Since the gasoline selectivity reached a certain level, excessive cracking of the products does not happen because the hydrogenolysis of Ru/CeO<sub>2</sub> is minimized by effective hydrocracking over the Ru/CeO<sub>2</sub> + BEA catalyst and the cracking of isomerized intermediates of gasoline-range hydrocarbons is not preferred over hydrogenation.<sup>20</sup> Similar trends in the hydroconversion reaction were observed according to the reaction time under a higher LDPE to catalyst ratio at 250 °C, as shown in Fig. S8(a). The catalytic activity was low in the early phase of hydroconversion and most of the LDPE reactants remained residual solid until 9 h. Then, the gasoline selectivity more than doubled from 18.3% at 9 h to 43.0% at 12 h, but still 30.3% of the unreacted polymer remained, possibly due to the viscous reaction melt and diffusion resistance. After 12 h, the catalytic performance of Ru/CeO<sub>2</sub> + BEA suddenly increased, with the yield

of solid residue and gasoline selectivity reaching 0.6% and 89.3% at 14 h, respectively. Thereafter, the product distribution seemed to equilibrate at 16 h, indicating that overcracking of gasoline into lighter hydrocarbons is unfavorable.<sup>20</sup> Furthermore, changes in the isomer fraction as a function of the reaction time were much clearer, as shown in Fig. S8(a). In the early stages until 9 h, the isomer fraction was low under 60%, which is not enough for effective  $\beta$ -scission. However, the isomer fraction at 12 h reached a saturated level of about 80%, which seems enough for the following active  $\beta$ -scission *via* hydrocracking. As a result, the catalytic activity rapidly increased to almost full conversion of LDPE and excellent gasoline selectivity. These results suggest that sufficient isomerization of reaction intermediates must precede the active hydroconversion of LDPE to gasoline-range hydrocarbons.

The effect of the initial hydrogen pressure on the catalytic performance of Ru/CeO<sub>2</sub> + BEA is shown in Fig. S8(b). A low methane yield (0.4–0.8%) was maintained across the entire hydrogen pressure range, indicating the ability of the dual catalyst to suppress methane production. The gasoline selectivity at 30–60 bar hydrogen pressure was approximately 96–97%. However, the C<sub>4</sub>–C<sub>7</sub> selectivity was about 50% at 30 bar and increased to about 56% as the initial hydrogen pressure increased to 50–60 bar. In addition, the color of the collected liquid product was light yellow at 30 bar and then turned transparent at 50–60 bar (Fig. S9). It seems that the cracking of the hydrocarbon chain and hydrogenation of the reaction intermediates are reduced at a hydrogen pressure of 30 bar and increased to a saturated value at more than 50 bar. This trend was much clearer under a low hydrogen pressure of 10 bar, with a reduction of LDPE conversion, gasoline selectivity, and C<sub>4</sub>–C<sub>7</sub> selectivity (Fig. S8) and a color change of the collected liquid products (Fig. S9). Meanwhile, it has been reported that competitive adsorption between the hydrocarbon reactant and hydrogen at the active metal sites could lead to the diminished depolymerization activity of PGM-based catalysts at excessive hydrogen pressure.<sup>53</sup> In contrast, the role of



the Ru metal in the Ru/CeO<sub>2</sub> + BEA hybrid catalyst is switched to the initial cracking of LDPE and hydrogenation of the reaction intermediates, so that the hybrid catalyst could remain active at high hydrogen pressure without competitive adsorption.

### Investigation of various zeolites in hybrid catalysts for LDPE hydroconversion

Various types of zeolites are commercially used in the catalytic cracking of crude oil, dewaxing process and hydroisomerization of liquid hydrocarbons.<sup>54–56</sup> According to their unique physicochemical properties such as surface area, pore diameter, hierarchical structure, crystal size and high surface acidity, the catalytic performance and product distribution are determined. The activity of various zeolites with similar Si/Al<sub>2</sub> ratios in the hybrid catalyst with Ru/CeO<sub>2</sub> in LDPE hydroconversion is examined and shown in Fig. 5. The physicochemical properties of various zeolites used are summarized in Table S5 and Fig. S10, S11. Among the various commercial zeolites, BEA (25) showed the highest activity with 98.8% of LDPE conversion and 95.4% of gasoline selectivity, followed by 84.2% of LDPE conversion and 76.4% of gasoline selectivity over Y(30) zeolite. ZSM-5(23) was also active in the dual catalyst, with almost full conversion of LDPE, 88.3% of gasoline selectivity and 11.4% of gaseous product selectivity. BEA-type zeolite has a large pore diameter and a macropore system with a three-dimensional cross-12-membered ring structure, which is suitable for hydrocracking of heavy oil.<sup>57</sup> Y-type zeolite also has a large pore diameter and open spaces in a supercage structure

of a 12-membered ring, which is conducive to the cracking of large molecular hydrocarbons. Furthermore, ZSM-5 has a unique pore structure with a 10-membered ring for shape-selective catalytic performance and is highly active for cracking processes.<sup>58</sup> Pyridine-IR revealed that Brønsted-to-Lewis acid site (BAS/LAS) ratios varied among the zeolites, with BEA at 0.73, Y at 0.61, and ZSM-5 at 2.23. BEA, Y, and ZSM-5 zeolites have three-dimensional pore structures in common, which reduce diffusion resistance and provide enough space for the isomerization and cracking of large hydrocarbon molecules.<sup>59</sup> These three-dimensional pore structures could result in relevant advantages in selective hydrocracking of large LDPE molecules into gasoline-range hydrocarbons over the hybrid catalysts. Meanwhile, ZSM-5 was less active in gasoline production than BEA with increased proportions of methane, ethane, and propane. This could originate from the increased influence of hydrogenolysis over hydrocracking due to the limited diffusion of large hydrocarbon molecules through the smaller pore diameters (5.4 Å of ZSM-5 and 7.4 Å of BEA, measured by N<sub>2</sub> adsorption-desorption). Also, as reported by Brenner *et al.*, the framework topology of ZSM-5 tunes the product distribution in the gas phase and increases the production of lighter hydrocarbons such as C<sub>3</sub> and C<sub>4</sub>.<sup>60</sup> These differences in the properties of the zeolites might lead to the change in C–C bond cracking over the hybrid catalyst, resulting in the increase of C<sub>3</sub> and C<sub>4</sub> production from 0.5 and 7.6% of BEA to 2.7 and 8.2% of ZSM-5, respectively.

Other commercial zeolites such as FER, SSZ-13 and MOR and amorphous SiO<sub>2</sub>-Al<sub>2</sub>O<sub>3</sub> were also examined in gasoline

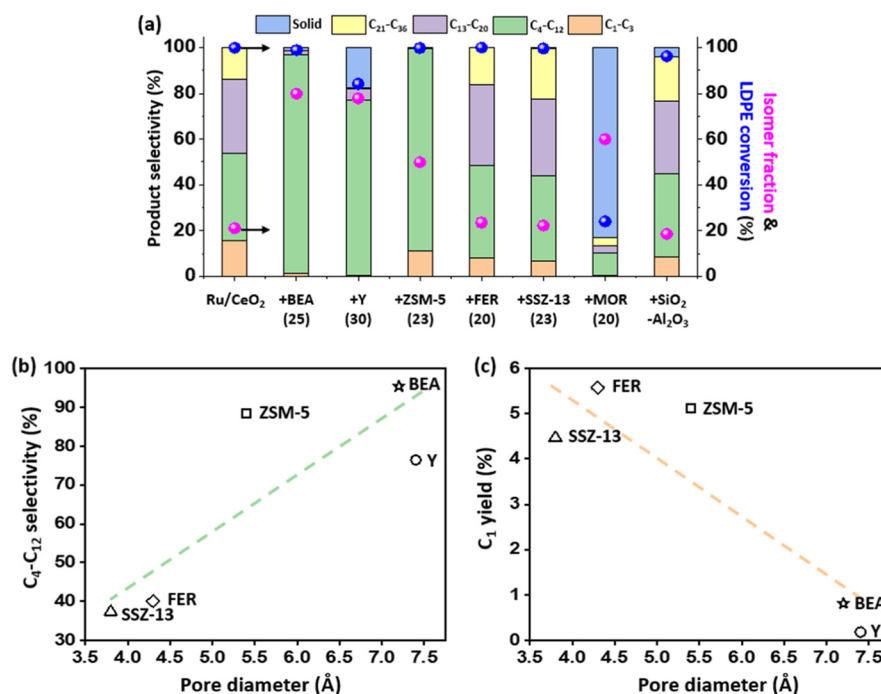


Fig. 5 (a) Product selectivity, LDPE conversion and isomer fraction in the gas and liquid products over various Ru/CeO<sub>2</sub> catalysts mixed with different zeolites. (b) Gasoline selectivity according to the pore diameter of zeolites. (c) Methane yield according to the pore diameter of zeolites. Reaction conditions: 3.5 g of LDPE, 0.25 g of catalysts, 260 °C, 50 bar H<sub>2</sub>, 4 h, mixing ratio of Ru/CeO<sub>2</sub> to zeolite = 1 : 2.



production when mixed with Ru/CeO<sub>2</sub>. Product distribution over the mixture catalysts with FER and SSZ-13 was similar to that of Ru/CeO<sub>2</sub> solely used, indicating that FER and SSZ-13 show no interaction with Ru/CeO<sub>2</sub> in LDPE hydroconversion. FER-type zeolite is known as an active catalyst in catalytic cracking of hydrocarbons with two-dimensional pore structures with 10-membered straight pores and 8-membered cross-pores.<sup>61</sup> Nonetheless, a small pore diameter of 4.3 Å in FER prohibits the diffusion of long-chain molecules and a series of skeletal rearrangement and β-scission could not be conducted at the acid sites in the micropore. SSZ-13 has a three-dimensional pore structure containing large cages of 7.3 Å and intersecting channels of 3.8 Å, making it quite active in the thermal cracking of ultra-high molecular weight PE at 400–500 °C.<sup>62</sup> However, the average diameter of the pore mouth in SSZ-13 is 3.8 Å, limiting the transfer of large molecules to the acid sites inside the small pore at a low temperature of 260 °C. Similarly, amorphous SiO<sub>2</sub>-Al<sub>2</sub>O<sub>3</sub> had no effect on the product distribution in the dual catalyst, probably due to the absence of a large pore diameter and structuralized pore system. Meanwhile, over the catalyst blend of Ru/CeO<sub>2</sub> and MOR zeolite with a one-dimensional pore structure, almost no conversion of LDPE was observed and most of the products remained unreacted. Even though the MOR has a large pore diameter (6.5 Å), abundant acid sites and high stability, its linearly arranged pore structure causes limited diffusion performance and slow discharge rate of long-chain hydrocarbons, thereby accelerating the deactivation of the catalyst even with small coking.<sup>63</sup> These results indicate that both the large pore diameter and the three-dimensional pore structure of the zeolite are crucial for the conversion of LDPE into recycled gasoline over the hybrid catalyst with Ru/CeO<sub>2</sub>.

In order to find the correlation of the physicochemical properties of zeolites with the catalytic activity in hybrid catalysts, gasoline selectivity over the various catalyst mixtures was plotted against total acidity measured by NH<sub>3</sub>-TPD, except for the catalyst with MOR (Fig. S10). FER had the most abundant acid sites on the surface, but the gasoline yield was low, and BEA, ZSM-5 and SSZ-13 had medium acidity, but BEA showed the highest gasoline selectivity while SSZ-13 exhibited the lowest gasoline selectivity. In spite of the smallest amount of acid sites in Y zeolite among the zeolites used, the high selectivity of gasoline was obtained in the mixture catalyst with Y. Considering the acidity of the zeolites with gasoline selectivity over the mixture catalysts, it seems that there is no correlation between gasoline selectivity and the amount of acid sites. By the way, gasoline selectivity and methane yield were compared with the pore diameter of the zeolites (Fig. 5b and c). Large pore zeolites (BEA and Y) showed high gasoline selectivity and suppressed production of methane, while small pore zeolites (FER and SSZ-13) showed low gasoline selectivity and large methane yield. Medium pore zeolite (ZSM-5) was active in gasoline production, but a large amount of gas products was produced as well. Therefore, it can be suggested that the pore size of the zeolite and enough space for hydrocracking are critical factors in the selective production of gasoline.

This assumption can also be confirmed by the amorphous SiO<sub>2</sub>-Al<sub>2</sub>O<sub>3</sub> with the highest acidity (0.501 mmol g<sup>-1</sup>) and small pore size (4.2 Å) that is not effective for gasoline production when mixed with Ru/CeO<sub>2</sub> (Fig. 5a).

In addition to zeolites, other widely used acidic catalysts such as Al<sub>2</sub>O<sub>3</sub> and WO<sub>3</sub>-TiO<sub>2</sub> were mixed with Ru/CeO<sub>2</sub> and their catalytic activities were examined in the LDPE hydroconversion reaction (Fig. S13). Ru/CeO<sub>2</sub> mixed with Al<sub>2</sub>O<sub>3</sub> and WO<sub>3</sub>-TiO<sub>2</sub> catalysts showed a small extent of increase in gasoline selectivity and the isomer fraction was similar to that of Ru/CeO<sub>2</sub> used solely. Al<sub>2</sub>O<sub>3</sub> and WO<sub>3</sub>-TiO<sub>2</sub> were not effective in the production of gasoline, indicating almost no synergistic effect with Ru/CeO<sub>2</sub> on the hydroconversion of LDPE. Al<sub>2</sub>O<sub>3</sub> had the largest pore diameter but its specific surface area and acidity were lower than those of BEA(25) (Fig. S14 and Table S6). WO<sub>3</sub>-TiO<sub>2</sub> also had a lower specific surface area, pore diameter and acidity than BEA(25). The poorer physicochemical properties of Al<sub>2</sub>O<sub>3</sub> and WO<sub>3</sub>-TiO<sub>2</sub>, as well as less organized pore structure, might explain the lower activity when mixed with Ru/CeO<sub>2</sub>.

Also, BEA zeolites with different acid densities, prepared from BEA with different Si/Al<sub>2</sub> ratios (25, 38 and 360), were blended with Ru/CeO<sub>2</sub> and their hydroconversion reaction was conducted (Fig. S15 and S16). BEA zeolites that have abundant surface acid sites were effective in producing gasoline-range hydrocarbons and suppressing methane yield. However, BEA with a low acidity of 0.090 mmol g<sup>-1</sup> showed no improvement over the Ru/CeO<sub>2</sub> + BEA, producing a broad product distribution. Since the C–C bond cleavage in long chain molecules mainly proceeded at the acid sites in the zeolite, the catalytic performance of the hybrid catalyst could be maximized over a sufficient amount of acid sites combined with the unique pore structure of the BEA zeolite.

### Comparison of the hybrid catalyst with Ru/BEA

Compared to the Ru/CeO<sub>2</sub> + BEA catalyst, another bifunctional hydrocracking catalyst with the combination of Ru and BEA, Ru/BEA (Ru loading = 5 wt%), was used in the LDPE hydroconversion reaction (Fig. 6). An equal amount of Ru was introduced into the reaction to compare the activity of each catalyst. Ru/BEA catalyzed 84.7% LDPE into liquid and gas products and its gasoline selectivity was 46.3%, with 71.0% of isomer fraction. Compared to Ru/CeO<sub>2</sub>, LDPE conversion was slightly decreased, possibly due to the difference in Ru particle size. As summarized in Table S7, the Ru particle size of Ru/BEA was twice larger than that of Ru/CeO<sub>2</sub>, despite its higher specific surface area, originating from the difference in metal–support interaction (MSI). This can also be inferred from XPS analysis (Fig. S17), where Ru species on the CeO<sub>2</sub> surface show higher binding energy than those on the BEA surface, due to the stronger interaction between the metal and the support in Ru/CeO<sub>2</sub>.<sup>22</sup> Nevertheless, gasoline selectivity and isomer fraction were improved over the Ru/BEA catalyst, indicating that the bifunctional hydrocracking mechanism of the Ru metal and acid sites in the zeolite is effective for selective gasoline production. According to the product distribution shown in



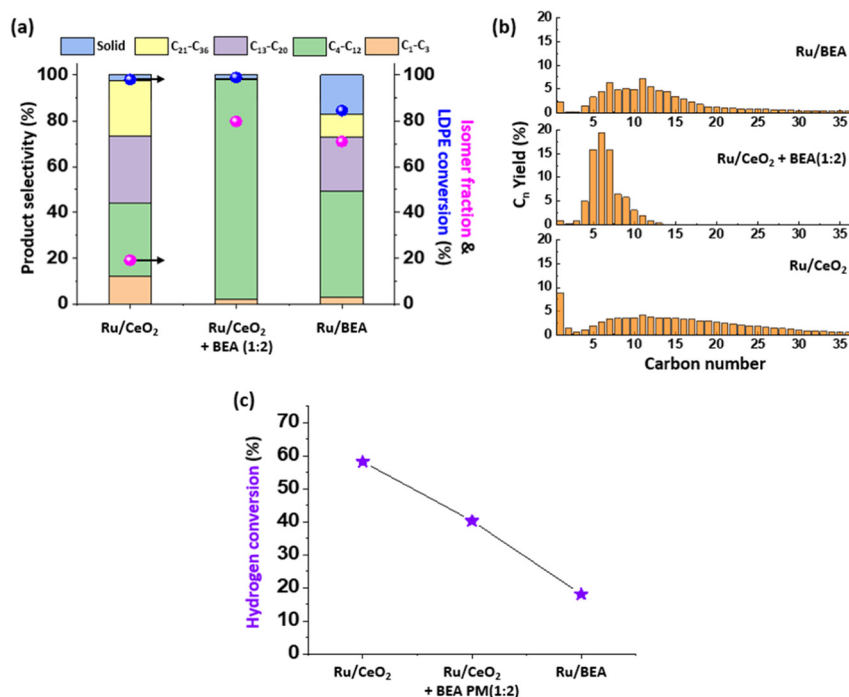


**Fig. 6** (a) Product selectivity, LDPE conversion and isomer fraction in the gas and liquid products, (b) product distribution, and (c) hydrogen conversion over Ru/CeO<sub>2</sub>, Ru/CeO<sub>2</sub> + BEA (1:2) and Ru/BEA catalysts. Reaction conditions: 3.5 g of LDPE, 0.083 g of Ru/CeO<sub>2</sub> and Ru/BEA catalysts, 0.25 g of Ru/CeO<sub>2</sub> + BEA (1:2) catalyst (equal amount of Ru introduced).

Fig. 6b, however, a broad liquid product distribution up to C<sub>36</sub> was obtained over the Ru/BEA catalyst, demonstrating that the hydrogenolysis pathway by the Ru metal is still influential over the Ru/BEA catalyst. This can also be confirmed by the unavoidable methane yield of 2.3% in Ru/BEA, due to the hydrogenolysis effect which is still influential. According to Jung *et al.*, excessive C–C cleavage by Ru could be promoted in Ru/BEA resulting from the prolonged residence time of reaction intermediates near Ru sites confined within micropores.<sup>50</sup> Limited access to active sites and the pore structure for effective  $\beta$ -scission as Ru was impregnated on BEA (Table S7) might be the other reasons for the enhanced hydrogenolysis. On the other hand, hydrocracking totally governs the hydroconversion reaction pathway over the Ru/CeO<sub>2</sub> + BEA catalyst, as evidenced by selective gasoline production with a high isomer fraction and suppressed methane yield. Separation of the Ru metal from the BEA zeolite is found to be more effective in hydrocracking of LDPE to gasoline. In addition, CeO<sub>2</sub> is a highly reducible support that is widely used in the reaction with hydrogen, while BEA is almost inactive in utilizing the hydrogen. As shown in Fig. 6c, hydrogen conversion was too high over Ru/CeO<sub>2</sub> and too low over Ru/BEA, respectively, implying that hydrogen is ineffectively used over Ru/CeO<sub>2</sub> and underutilized over Ru/BEA in LDPE hydroconversion. Conversely, it seems that Ru/CeO<sub>2</sub> + BEA could effectively utilize hydrogen to selectively produce gasoline with a medium degree of hydrogen consumption. Moreover, coke species on the post-reaction catalysts were analyzed by TGA (Fig. S18). To

effectively separate the post-reaction catalysts from the reactants and rule out the impact of unreacted LDPE, we conducted a model hydroconversion reaction using octadecane (C<sub>18</sub>) (Fig. S19). As shown in Fig. S18, a decrease in sample weight below 200 °C corresponds to the desorption of moisture and light gaseous molecules and weight change above 200 °C was used to analyze coke formation.<sup>64</sup> The amount of coke species in Ru/CeO<sub>2</sub> + BEA was 4.56% and that in Ru/BEA was 4.63%. A similar amount of coke was deposited on both catalysts, indicating that the effect of lower intimacy between Ru and acid sites in Ru/CeO<sub>2</sub> + BEA could be alleviated by impregnating Ru on highly reducible metal oxide (CeO<sub>2</sub>), which promotes hydrogenation of reaction intermediates and suppresses coke formation on BEA. It can be suggested that by simply mixing Ru/CeO<sub>2</sub> and BEA, the reaction pathway and the extent of hydrogen utilization can be controlled to maximize the production of liquid hydrocarbons within a target range.

To further discuss the role of CeO<sub>2</sub> and BEA in mixture catalysts, LDPE hydroconversion over the dual catalyst with Ru/BEA and pristine BEA or CeO<sub>2</sub> was conducted (Fig. S20). Using the same amount of Ru/BEA, addition of pristine BEA increased gasoline selectivity and isomer fraction in the liquid products and suppressed the production of methane. It can also be confirmed in Ru/BEA + BEA that pristine BEA could reduce the effect of hydrogenolysis by Ru/BEA and switch the reaction pathway to hydrocracking. Meanwhile, to take the function of CeO<sub>2</sub> into account, pristine CeO<sub>2</sub> was mixed with Ru/BEA. Although CeO<sub>2</sub> alone showed no activity in LDPE



hydroconversion (data not shown), the degradation activity of Ru/BEA + CeO<sub>2</sub> was increased to almost full conversion of LDPE and 85% gasoline selectivity, indicating some synergies between Ru/BEA and pristine CeO<sub>2</sub>. However, gasoline selectivity and isomer fraction over Ru/BEA + CeO<sub>2</sub> were lower than those of Ru/CeO<sub>2</sub> + BEA. Moreover, the undesired methane yield increased to 8.0%. This methane production is not suppressed by adding additional pristine BEA over Ru/BEA + CeO<sub>2</sub> (Ru/BEA + CeO<sub>2</sub>, BEA (1 : 1 : 1) catalyst, which contains equal amounts of Ru, CeO<sub>2</sub> and BEA compared to the Ru/CeO<sub>2</sub> + BEA (1 : 2) catalyst). It can be inferred from these results that the LDPE hydroconversion pathway over Ru/BEA + CeO<sub>2</sub> is slightly different compared to Ru/CeO<sub>2</sub> + BEA and methane is produced through a pathway other than hydrogenolysis over Ru/CeO<sub>2</sub>. A sudden increase in hydrogen conversion over Ru/BEA + CeO<sub>2</sub> also assures partial changes in the reaction pathway. As previously mentioned, CeO<sub>2</sub> is a highly reducible material which can store the adsorbed hydrogen atom through hydrogen spillover. In the H<sub>2</sub>-TPR profiles of CeO<sub>2</sub> and BEA supported Ru catalysts (Fig. S21), pristine CeO<sub>2</sub> shows two reduction peaks at 400–600 °C and over 750 °C, which correspond to the reduction of surface oxygen and bulk oxygen in CeO<sub>2</sub>, respectively. Disappearance of the reduction peak of surface oxygen in Ru/CeO<sub>2</sub> catalysts, as well as the lowered reduction temperature of the bulk oxygen peak, indicates the hydrogen spillover from the Ru metal to the CeO<sub>2</sub> surface. In Ru/BEA + CeO<sub>2</sub>, the reduction peak of surface oxygen in CeO<sub>2</sub> disappeared as well, which shows the transfer of hydrogen from Ru on BEA to physically mixed CeO<sub>2</sub>.<sup>65</sup> This increase in the utilization of hydrogen by pristine CeO<sub>2</sub> might be related to the improved LDPE conversion and gasoline selectivity; however, undesired methane production follows as well. It can be suggested from these results that the best catalytic design for selective gasoline production without methane in LDPE hydroconversion is impregnating Ru metal on the CeO<sub>2</sub> support and blending with pristine BEA.

### Catalytic degradation of various PE and PP feeds over hybrid catalysts and catalyst reusability

Polyolefin polymers have different structures (linear or branched), average molecular weight, crystallinity, and viscosity in the melt phase. To investigate the applicability of the hybrid catalyst to the hydroconversion of various PE and PP feeds, a variety of commercial PE and PP samples were obtained from Sigma-Aldrich (Fig. S22), and their degradation reactions were conducted over Ru/CeO<sub>2</sub> + BEA (Fig. 7). The hybrid catalyst was highly active in the depolymerization of PE with high molecular weight. In addition, more methane is generally produced in PP degradation through the terminal C–C bond cracking of abundant methyl groups compared to PE degradation.<sup>15</sup> Ru/CeO<sub>2</sub> + BEA was also effective in selective gasoline production from PP with minimized methane production. A small amount of solid residue in HDPE and LLDPE hydroconversion may come from the different viscosities and liquidities of the melt phase,<sup>41</sup> but the gasoline selectivity remained high. These results indicate that the synergistic

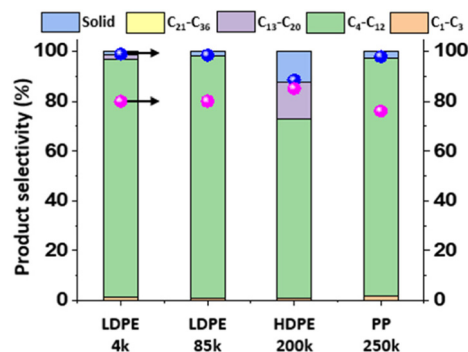


Fig. 7 Product selectivity, LDPE conversion and isomer fraction in the gas and liquid products from the hydroconversion of various PE and PP feeds over Ru/CeO<sub>2</sub> + BEA. Reaction conditions: 3.5 g of feeds, 0.25 g of catalyst, 260 °C, 50 bar H<sub>2</sub>, 4 h, mixing ratio of Ru/CeO<sub>2</sub> to BEA = 1 : 2.

effect of Ru/CeO<sub>2</sub> and BEA could lead to selective gasoline production from various PE and PP feeds, and the hybrid catalyst shows the flexibility to tackle various types of real-world plastics.

The reusability test of Ru/CeO<sub>2</sub> + BEA was conducted with the post-reaction catalyst, and the results are summarized in Fig. S23. Unfortunately, the post-reaction Ru/CeO<sub>2</sub> + BEA was deactivated and the catalytic activity was not recovered after the regeneration. When the post-reaction Ru/CeO<sub>2</sub> was reused under the same reaction conditions, almost the same performance was observed, indicating that Ru/CeO<sub>2</sub> is not a main reason for Ru/CeO<sub>2</sub> + BEA deactivation. Coke deposition on BEA might be the critical factor, and although the coke deposition on BEA could be removed during regeneration, the activity of regenerated Ru/CeO<sub>2</sub> + BEA was not fully recovered, possibly due to the sintering of Ru. To deal with this problem, fresh BEA was introduced to the post-reaction Ru/CeO<sub>2</sub> + BEA without regeneration and the catalytic activity was fully restored. It can be inferred from these results that coke deposition on BEA critically affects the activity of the post-reaction catalyst and we could enable the reusability of Ru/CeO<sub>2</sub> + BEA by the addition of fresh acid catalysts.

## Conclusions

In this study, a bifunctional hybrid catalyst of Ru/CeO<sub>2</sub> and BEA zeolite was found to be highly active in LDPE hydroconversion. The synergistic effect between Ru/CeO<sub>2</sub> and BEA resulted in the selective production of gasoline-range hydrocarbons (95.4%) with a large fraction of branched products and suppressed methane yield (<0.8%). Also, an adequate mixing ratio of Ru/CeO<sub>2</sub> and BEA is crucial not only for maximizing the gasoline yield but also to ensure high quality of liquid products. The Ru/CeO<sub>2</sub> and BEA hybrid catalyst demonstrated a highest productivity of 3451 g<sub>C<sub>5</sub>-C<sub>12</sub></sub> g<sub>Ru</sub><sup>-1</sup> h<sup>-1</sup> among the recently reported Ru-based hydroconversion catalysts, and this was even higher than that of Pt and Ir-based hydrocracking catalysts in the literature. The influence of various reaction para-



meters on LDPE hydroconversion over the catalyst mixture was investigated; BEA addition into Ru/CeO<sub>2</sub> resulted in a change in the reaction pathway from hydrogenolysis to hydrocracking, which is relevant in selective gasoline production from a minimum reaction temperature of 250 °C. When the activity of Ru/CeO<sub>2</sub> with various zeolites and acidic catalysts was evaluated, it was found that not just the high surface acidity but also the combination of the three-dimensional large pore structure with sufficient acidity in BEA was essential for selective gasoline production, and a linear correlation of gasoline selectivity and methane yield with the pore diameter of the zeolites was found to be important. Moreover, another bifunctional catalyst of Ru with BEA, Ru/BEA, was less active in LDPE conversion and gasoline production, and Ru/CeO<sub>2</sub> + BEA was found to be more active in LDPE hydroconversion. These insights discussed in this study could contribute to the efficacious design of bifunctional catalysts, resulting in the efficient production of fuel-range hydrocarbons from polyolefins with heterogeneous catalysts.

## Author contributions

J. S. conducted most of the experiments and data analysis of the research; J. S., H. J. and D. H. K. designed the experiments; D. H. K. supervised the project and acquired the funding; D. H. K., J. S. C., J. B. and H. J. reviewed and revised the manuscript; and all authors discussed the results.

## Conflicts of interest

The authors declare no conflict of interest.

## Data availability

The data that support the findings of this study are available in the main text and the supplementary information (SI). Supplementary information is available. See DOI: <https://doi.org/10.1039/d6gc00351f>.

## Acknowledgements

This research was supported by LG Chem. and the Basic Science Research Program through the National Research Foundation of Korea (NRF) funded by the Ministry of Science, ICT & Future Planning (MSIP, NRF-RS-2025-00519715). The Institute of Engineering Research at Seoul National University partially provided research facilities for this study.

## References

- 1 F. Khan, W. Ahmed and A. Najmi, *Resour., Conserv. Recycl.*, 2019, **142**, 49–58.
- 2 G. C. N. T. Pilapitiya and A. S. Ratnayake, *Cleaner Mater.*, 2024, **11**, 100220.
- 3 R. Geyer, *Plastic Waste and Recycling*, 2020, ch. 2, pp. 13–32.
- 4 A. J. Martín, C. Mondelli, S. D. Jaydev and J. Pérez-Ramírez, *Chem*, 2021, **7**, 1487–1533.
- 5 A. L. Jadhav, P. A. Gardi and P. A. Kadam, *Korean J. Chem. Eng.*, 2024, **41**, 2937–2960.
- 6 H. Almohamadi, M. Alamoudi, U. Ahmed, R. Shamsuddin and K. Smith, *Korean J. Chem. Eng.*, 2021, **38**, 2208–2216.
- 7 A. Tennakoon, X. Wu, A. L. Paterson, S. Patnaik, Y. C. Pei, A. M. LaPointe, S. C. Ammal, R. A. Hackler, A. Heyden, I. I. Slowing, G. W. Coates, M. Delferro, B. Peters, W. Y. Huang, A. D. Sadow and F. A. Perras, *Nat. Catal.*, 2020, **3**, 893–901.
- 8 S. Belbessai, A. Azara and N. Abatzoglou, *Processes*, 2022, **10**, 733.
- 9 Chevron, *Motor Gasoline Technical Review*, Chevron Corporation, 2016.
- 10 J. Zhao, Y. J. Zheng and Z. P. Zhang, *Anal. Methods*, 2020, **12**, 1926–1934.
- 11 IEA, *Oil 2023: Analysis and forecast to 2028*, IEA, International Energy Agency (IEA), Paris, 2023. <https://www.iea.org/reports/oil-2023>.
- 12 J. Y. Xin, D. X. Yan, O. Ayodele, Z. Zhang, X. M. Lu and S. J. Zhang, *Green Chem.*, 2015, **17**, 1065–1070.
- 13 A. Brown and P. Börkey, *OECD Environment Working Papers*, 2024, **236**, 1–50.
- 14 K. Tumu, K. Vorst and G. Curtzwiler, *J. Environ. Manage.*, 2023, **348**, 119242.
- 15 Y. Nakaji, M. Tamura, S. Miyaoka, S. Kumagai, M. Tanji, Y. Nakagawa, T. Yoshioka and K. Tomishige, *Appl. Catal., B*, 2021, **285**, 119805.
- 16 S. D. Jaydev, A. J. Martín and J. Pérez-Ramírez, *ChemSusChem*, 2021, **14**, 5179–5185.
- 17 P. A. Kots, S. B. Liu, B. C. Vance, C. Wang, J. D. Sheehan and D. G. Vlachos, *ACS Catal.*, 2021, **11**, 8104–8115.
- 18 S. L. Lu, Y. X. Jing, S. C. Jia, M. Shakouri, Y. F. Hu, X. H. Liu, Y. Guo and Y. Q. Wang, *ChemCatChem*, 2023, **15**, e202201375.
- 19 C. Wang, T. J. Xie, P. A. Kots, B. C. Vance, K. W. Yu, P. Kumar, J. Y. Fu, S. B. Liu, G. Tsilomelekis, E. A. Stach, W. Q. Zheng and D. G. Vlachos, *JACS Au*, 2021, **1**, 1422–1434.
- 20 J. C. Yan, G. N. Li, Z. W. Lei, X. L. Yuan, J. T. Li, X. R. Wang, B. Wang, F. P. Tian, T. Hu, L. Huang, Y. J. Ding, X. K. Xi, F. Zhu, S. Zhang, J. Li, Y. Chen, R. G. Cao and X. Wang, *Nat. Commun.*, 2025, **16**, 2800.
- 21 T. Kim, H. Nguyen-Phu, T. Kwon, K. H. Kang and I. Ro, *Environ. Pollut.*, 2023, **331**, 121876.
- 22 L. X. Chen, L. C. Meyer, L. Kovarik, D. Meira, X. I. Pereira-Hernandez, H. H. Shi, K. Khivantsev, O. Y. Gutiérrez and J. Szanyi, *ACS Catal.*, 2022, **12**, 4618–4627.
- 23 A. Tomer, M. M. Islam, M. Bahri, D. R. Inns, T. D. Manning, J. B. Claridge, N. D. Browning, C. R. A. Catlow, A. Roldan, A. P. Katsoulidis and M. J. Rosseinsky, *Appl. Catal., A*, 2023, **666**, 119431.



- 24 J. E. Rorrer, A. M. Ebrahim, Y. Questell-Santiago, J. Zhu, C. Troyano-Valls, A. S. Asundi, A. E. Brenner, S. R. Bare, C. J. Tassone, G. T. Beckham and Y. Roman-Leshkov, *ACS Catal.*, 2022, **12**, 13969–13979.
- 25 M. Y. Sun, L. J. Zhu, W. Liu, X. P. Zhao, Y. F. Zhang, H. Luo, G. Miao, S. G. Li, S. Yin and L. Z. Kong, *Sustainable Energy Fuels*, 2022, **6**, 271–275.
- 26 H. K. Wang, T. Yoskamtorn, J. W. Zheng, P. L. Ho, B. Ng and S. C. E. Tsang, *ACS Catal.*, 2023, **13**, 15886–15898.
- 27 Z. Ma, Z. B. Zhang, C. Y. Wang, J. L. Cao, Y. B. Liu, H. Yan, X. Zhou, X. Feng and D. Chen, *Green Chem.*, 2025, **27**, 1169–1182.
- 28 H. Kim, Y. H. Lim, J. H. Park, J. M. Ha and D. H. Kim, *Green Chem.*, 2024, **26**, 2692–2704.
- 29 I. Song, H. Lee, S. W. Jeon, I. A. M. Ibrahim, J. Kim, Y. Byun, D. J. Koh, J. W. Han and D. Kim, *Nat. Commun.*, 2021, **12**, 901.
- 30 S. B. Liu, P. A. Kots, B. C. Vance, A. Danielson and D. G. Vlachos, *Sci. Adv.*, 2021, **7**, eabf8283.
- 31 L. Li, H. Luo, Z. L. Shao, H. Z. Zhou, J. W. Lu, J. J. Chen, C. J. Huang, S. A. Zhang, X. F. Liu, L. Xia, J. Li, H. Wang and Y. H. Sun, *J. Am. Chem. Soc.*, 2023, **145**, 1847–1854.
- 32 K. Faust, P. Denifl and M. Hapke, *ChemCatChem*, 2023, **15**, e202300310.
- 33 E. Stauffer, J. A. Dolan and R. Newman, *Fire Debris Analysis*, Academic Press, 2008.
- 34 N. S. Almuqati, A. M. Aldawsari, K. N. Alharbi, S. González-Cortés, M. F. Alotibi, F. Alzaidi, J. R. Dilworth and P. P. Edwards, *Fuel*, 2024, **366**, 131270.
- 35 F. Pradelle, S. L. Braga, A. R. F. A. Martins, F. Turkovics and R. N. C. Pradelle, *Energy Fuels*, 2015, **29**, 7753–7770.
- 36 B. Fanget, A. Koudil, R. Corroyer, A. Pagot and J. Fernandes, Process for the production of light olefins and BTX using a catalytic cracking unit, ncc, processing a naphtha type feed, a catalytic reforming unit and an aromatics complex, *IFP Energies Nouvelles*, FR1453076A, 2014.
- 37 Z. D. Luo, H. Y. Wang, K. Chen, J. Liu, C. L. Wu and Z. Wei, *Int. J. Polym. Anal. Charact.*, 2015, **20**, 240–249.
- 38 X. D. Jing, G. X. Yan, Y. H. Zhao, H. Wen and Z. H. Xu, *Polym. Degrad. Stab.*, 2014, **109**, 79–91.
- 39 L. C. Jones and L. W. Taylor, *Anal. Chem.*, 1955, **27**, 228–237.
- 40 Q. Du, X. Shang, Y. Y. Yuan, X. Su and Y. Q. Huang, *Catalysts*, 2025, **15**, 335.
- 41 M. Tamura, S. Miyaoka, Y. Nakaji, M. Tanji, S. Kumagai, Y. Nakagawa, T. Yoshioka and K. Tomishige, *Appl. Catal., B*, 2022, **318**, 121870.
- 42 W. T. Lee, A. van Muyden, F. D. Bobbink, M. D. Mensi, J. R. Carullo and P. J. Dyson, *Nat. Commun.*, 2022, **13**, 4850.
- 43 S. D. Jaydev, A. J. Martín, M. E. Usteri, K. Chikri, H. Eliasson, R. Erni and J. Pérez-Ramírez, *Angew. Chem., Int. Ed.*, 2024, **63**, e202317526.
- 44 Q. Y. Kang, M. Y. Chu, P. P. Xu, X. C. Wang, S. Q. Wang, M. H. Cao, O. Ivasenko, T. K. Sham, Q. Zhang, Q. M. Sun and J. X. Chen, *Angew. Chem., Int. Ed.*, 2023, **62**, e202313174.
- 45 A. Bin Jumah, V. Anbumuthu, A. A. Tedstone and A. A. Garforth, *Ind. Eng. Chem. Res.*, 2019, **58**, 20601–20609.
- 46 X. Wu, A. Tennakoon, R. Yappert, M. Esveld, M. S. Ferrandon, R. A. Hackler, A. M. LaPointe, A. Heyden, M. Delferro, B. Peters, A. D. Sadow and W. Y. Huang, *J. Am. Chem. Soc.*, 2022, **144**, 5323–5334.
- 47 X. T. Wu, X. Wang, L. L. Zhang, X. M. Wang, S. Y. Song and H. J. Zhang, *Angew. Chem., Int. Ed.*, 2024, **63**, e202317594.
- 48 B. W. Du, X. Chen, Y. Ling, T. T. Niu, W. X. Guan, J. P. Meng, H. Q. Hu, C. W. Tsang and C. H. Liang, *ChemSusChem*, 2023, **16**, e202202035.
- 49 J. Q. Cao, X. B. Gong, S. Li, Y. W. Wang, X. Feng, J. Gao and S. Shi, *ChemCatChem*, 2025, **18**, e01358.
- 50 H. Jung, J. Suh, Y. H. Lim, H. Kim, I. Song, E. Lee, J. S. Choi, J. Bang and D. Kim, *Chem. Eng. J.*, 2026, **530**, 173480.
- 51 V. Calemme, S. Peratello and C. Perego, *Appl. Catal., A*, 2000, **190**, 207–218.
- 52 M. Zare, D. Sahseh, O. H. Bamidele and A. Heyden, *Chem Catal.*, 2024, **4**, 101093.
- 53 J. E. Rorrer, C. Troyano-Valls, G. T. Beckham and Y. Román-Leshkov, *ACS Sustain. Chem. Eng.*, 2021, **9**, 11661–11666.
- 54 H. Kang, J. Yoon, D. W. Jun, K. H. Kang, I. Ro, S. Jeong and J. H. Kang, *Commun. Eng.*, 2025, **4**, 57.
- 55 L. S. Wei, H. Wang, Q. Dong, Y. W. Li and H. W. Xiang, *Catalysts*, 2025, **15**, 401.
- 56 T. Kwon, J. Park, K. H. Kang, D. S. Jung, W. Won and I. Ro, *Green Chem.*, 2025, **27**, 11769–11781.
- 57 Z. L. Hu, T. T. Wu, H. D. Xie, Y. T. Zhang, S. D. Ge and Z. J. Wu, *Chem. Eng. J.*, 2024, **499**, 155761.
- 58 A. Kostyniuk, D. Bajec and B. Likozar, *Appl. Catal., A*, 2021, **612**, 118004.
- 59 Y. He, J. J. Chen, D. D. Li, Q. Zhang, D. X. Liu, J. Y. Liu, X. Q. Ma and T. J. Wang, *Energy*, 2021, **223**, 120046.
- 60 A. E. Brenner, G. Drake, G. T. Beckham and Y. Román-Leshkov, *JACS Au*, 2025, **5**, 4123–4132.
- 61 P. del Campo, C. Martínez and A. Corma, *Chem. Soc. Rev.*, 2021, **50**, 8511–8595.
- 62 J. R. S. Solano, R. C. S. Nascimento, D. C. M. Silva, D. P. S. Silva, L. V. Sousa, B. J. B. Silva, S. L. Alencar, M. M. Urbina, P. H. L. Quintela and A. O. S. Silva, *Mater. Res.*, 2021, **24**, e20210066.
- 63 M. G. Shelyapina, *Molecules*, 2024, **29**, 5432.
- 64 A. Hart, M. Adam, J. P. Robinson, S. P. Rigby and J. Wood, *Top. Catal.*, 2020, **63**, 268–280.
- 65 E. W. Lee, J. H. Lee, S. Hwang and D. Kim, *J. Catal.*, 2023, **417**, 421–431.

